Implication of tropical lower stratospheric cooling in recent trends in tropical circulation and deep convective activity

Kunihiko Kodera[1], Nawo Eguchi[2], Rei Ueyama[3], Yuhji Kuroda[1,4], Chiaki Kobayashi[1], Beatriz M. Funatsu[5], Chantal Claud[6]

[1] Meteorological Research Institute, Tsukuba, 305-0052, Japan

[2] Research Institute for Applied Mechanics, Kyushu University, Kasuga, 816-8580, Japan

[3] NASA Ames Research Center, Moffett Field, 94035-0001, USA

[4] Meteorological College, Kashiwa, Japan

[5] CNRS, Université de Nantes, UMR 6554 LETG, Campus du Tertre, Nantes, 44312, France

[6] Laboratoire de Météorologie Dynamique, Ecole Polytechnique, Palaiseau, 91128, France

Correspondence to: Kunihiko Kodera (kodera.kk@gmail.com).

Abstract. Large changes in tropical circulation from the mid-to-late 1990s to the present, in particular changes related to the summer monsoon and cooling of the sea surface in the equatorial eastern Pacific, are noted. The cause of such recent decadal variations in the tropics was studied using a meteorological reanalysis dataset. Cooling of the equatorial southeastern Pacific Ocean occurred in association with enhanced cross-equatorial southerlies, which resulted from a strengthening of the deep ascending branch of the boreal summer Hadley circulation over the continental sector connected to stratospheric circulation. From boreal summer to winter, the anomalous convective activity centre moves southward following the seasonal march to the equatorial Indian Ocean–Maritime Continent region, which strengthens the surface easterlies over the equatorial central Pacific. Accordingly, ocean surface cooling extends over the equatorial central Pacific. We suggest that the fundamental cause of the recent decadal change in the tropical troposphere and the ocean is a poleward shift of convective activity that resulted from a strengthening of extreme deep convection penetrating into the tropical tropopause layer, particularly over the African and Asian continents and adjacent oceans. We conjecture that the increase in extreme deep convection is produced by a combination of land surface warming due to increased CO_2 and a reduction of static stability in the tropical tropopause layer due to tropical stratospheric cooling.

1 Introduction

Large changes in tropical circulation occurred from the mid-to-late 1990s to the present, in particular changes related to the summer monsoon and cooling of the sea surface in the equatorial eastern Pacific, are noted. Such a decrease in the tropical

east Pacific sea surface temperature (SST) has been associated with a slowdown, or hiatus, of global warming (Kosaka and Xie, 2013; England et al., 2014; Trenberth et al., 2014; Watanabe et al., 2014). Changes were also found in the advancement of the onset of the Asian summer monsoon (Kajikawa et al., 2012; Gautam and Regmi, 2013; Xiang and Wang, 2013; Yun et al., 2014) and an increase in precipitation over the Sahel in West Africa (Fontaine et al., 2011; Brandt et al., 2014; Maidment et al., 2015; Diawara et al., 2016). An increase in precipitation in southern Africa was also observed during austral summer (Vizy and Cook, 2016). In addition to these large-scale circulation changes, variations occurred in mesoscale phenomena such as an increase in Mesoscale Convective Systems (MCSs) over the Sahel (Taylor et al., 2017). A relationship between tropopause layer cooling and tropical cyclone activity in the Atlantic has also been suggested (Emanuel et al., 2013 Indeed, recent numerical model studies show that cooling of the tropopause, as well as SSTs, impacts the intensity of tropical storms (Ramsay, 2013; Wang et al., 2014). In this respect, the recent cooling of the tropical tropopause and lower stratosphere from around 2000 (Randel et al., 2006; Randel and Jensen, 2013) should be investigated together with tropical tropospheric change.

The importance of the Pacific Decadal Oscillation (PDO) to decadal changes in global temperature and precipitation has been noted previously (Meehl et al., 2013; Dong and Dai, 2015; Trenberth, 2015). The most recent hiatus in global warming ended around 2013 followed by a strong warming due to an El Niño event in 2015 (Hu and Fedorov, 2017; Liu and Zhou, 2017; Urabe et al., 2017; Xie and Kosaka, 2017). However, the El Niño of 2015/16 differed from the large 1997/98 El Niño, which involved less warming in the eastern Pacific (Paek et al., 2017), conforming to a trend of increasing intensity of central Pacific-type El Niños (Kao and Yu, 2009; Johnson, 2013). In this sense, the anomalous tropical circulation from the mid-to-late 1990s did not terminate with the hiatus around 2013, but still persists today. Similarly, the northward shift of the convective zone in boreal summer continues, as shown below.

Multidecadal variations in the atmosphere–ocean coupled mode, such as the Atlantic Multidecadal Oscillation, have also been proposed as a cause of recent changes in tropics (Wang et al., 2013; Kamae et al., 2017). Kamae et al. (2017) studied the impact of SSTs in various oceanic basins on recent trends in monsoon precipitation using a coupled ocean model. They were able to reproduce the recent increasing trend in monsoon rainfall in the Northern Hemisphere (NH), except for the Asian monsoon, with changes in Atlantic SST. Atlantic SSTs, however, have practically no effect on the African or Australian monsoons in the Southern Hemisphere (SH). Another difference from observations is that the simulated increase in rainfall occurs mainly over the oceans and at low latitudes between the equator and 15°N rather than the observed increase over continents between around 10°N and 20°N (see fig. 3 of Kamae et al., 2017). Thus, it is difficult to attribute recent global trends to a regional mode of decadal oceanic variation alone. In this paper, we suggest that the fundamental cause of the recent decadal trend in the tropics from around 1999 is not the PDO, but rather a strengthening of the deep ascending branch of the summertime Hadley circulation extending into the stratosphere.

One of the components of the recent tropical circulation change is an expansion of the tropics (e.g., Davis and Rosenlof, 2012; Lucas et al., 2013; Hu et al., 2018; Byrne et al., 2018). Tropical expansion has been linked to changes in the descending branch of the Hadley cell in the subtropics (Kang and Polvani, 2011), but other potential mechanisms include changes in SST and in the vertical temperature structure of the troposphere, an overall increase in tropopause height, the internal variability of the climate system, and possibly stratospheric climate change (Seidel et al,. 2007). Among the studies on tropical expansion those on the role of the tropical SST (Allen et al., 2018; Amaya et al., 2018) may be relevant to the present study. However, as will be shown later, a decadal ocean variability such as PDO may not be a fundamental factor which produces recent decadal trend in boreal summer. For the purposes of this paper we assume that the changes that we discuss are not directly related to those associated with tropical expansion.

Global climate change involves diverse aspects from the stratosphere to the ocean, from the polar region to the tropics, and from monsoons to severe storms. Each of these elements should be investigated independently in great detail, as well as their relationships to each other and their roles in global climate change. Without the latter, we will be unable to see the 'big picture.' Stratospheric variation has generally been treated as a problem separate from recent surface climate change. The goal of this study is to provide a framework for assembling these diverse pieces of the climate-change puzzle by investigating the connection between the atmosphere and ocean in the tropics.

The remainder of this paper is organized as follows. The data used in this study are presented in section 2, and the results of our analysis are given in section 3. A summary and discussion of the causes of recent climate changes in tropics are presented in section 4.

2 Data

We use meteorological reanalysis data produced by the Japan Meteorological Agency (JMA), JRA55 (Kobayashi et al., 2015). A large discontinuity was found at the end of the 1990s in a previous reanalysis product, JRA25, when the TIROS Operational Vertical Sounder (TOVS) onboard the National Oceanic and Atmospheric Administration (NOAA) satellite was switched to Advanced TOVS (ATOVS; Li et al., 2000). This discontinuity has largely been removed in the JRA55 reanalysis (Kobayashi et al., 2015).

Outgoing longwave radiation (OLR) data provided by NOAA are widely used in analyses of convective activity in the tropics. In the present study, we use monthly mean OLR data (1° × 1° latitude–longitude resolution) derived from the High-Resolution Infrared Radiation Sounder (HIRS) (Lee et al., 2007), available at ftp://eclipse.ncdc.noaa.gov/cdr/hirs-olr/monthly/. An analysis of the precipitation is performed using Global Precipitation Climatology Project (GPCP) monthly

mean data version 2.3 (Adler et al., 2003). Monthly mean gridded SST data from COBE with $1° \times 1°$ grid cells compiled by the JMA (Ishii et al., 2005) are used for the study of ocean surface change.

In the case of extreme deep convection, strong updraft further penetrates beyond the level of neutral buoyancy and overshoots into the tropical tropopause layer (TTL). Such tropical overshooting clouds (COV) were identified using the diagnostics developed by Hong et al. (2005), which are based on brightness temperature differences measured by three high-frequency channels of the Advanced Microwave Sensing Unit (AMSU) module B or the Microwave Humidity Sensor (MHS). Data are from NOAA and MetOp satellites with periods of 2007–2013 for MetOp-A and 2014–2017 for MetOp-B. Their equatorial crossing times are nearly identical (see fig. 1 of Funatsu et al., 2016). The original data calculated on a $0.25°$ $\times\ 0.25°$ grid were resampled to a coarse one of $2.25° \times 2.25°$ grid for plotting. The number density of COV is defined as the total number of COV detected in each $2.25° \times 2.25°$ bin divided by the MetOp–MHS total pixel number to remove sampling bias, with units of parts-per-thousand.

The climatology is defined here as the 30-year mean from 1981 to 2010. The exact starting dates of the recent decadal change is difficult to determine on the one hand due to the interannual variability (such as the El Niño events), and variable dependent characteristics of change. For example, while some variables show a stepwise transition, others show a more gradual change. In the present study, we define the recent decadal change as the 1999-2016 mean anomalies from the 30-year (1981-2010) mean unless otherwise specified. By selecting the year 1999 as the starting year, we excluded the extremely large 1997/98 El Niño event from the recent period.

Seven El Niño events after 1979 are identified by the JMA based on 6-monthly mean SSTs in the Niño 3 sector (5° S–5° N, 150° W–90° W; available at http://ds.data.jma.go.jp/gmd/tcc/tcc/products/elnino/ensoevents.html). In this study, we define the NH cold seasons of 1982/83, 1986/87, 1991/92, 1997/98, 2002/03, 2009/10, and 2015/16 as El Niño winters. The choice of the year 1999 was made to exclude the extremely large 1997/98 El Niño event from the recent period.

3 Results

3.1 Recent decadal change

The recent change of tropical convective activity is identified from the July–September 1999-2016 mean anomalous OLR relative to the 30-year climatology (1981–2010) (Fig. 1a). Increase in convective activity occurs over the African and Asian summer monsoon regions. Deep convective activity reaching the TTL in boreal summer is located primarily over the continents and their adjacent ocean north of 10° N (see e.g., Fig 2 in Liu and Zipser, 2005). It should be noted that the climatological mean stream lines around 15° N are connected to the stratosphere by crossing the tropopause (100 hPa) in boreal summer (see e.g., Fig 3 of Seviour et al., 2012). In the present study, we call this part of the ascending branch of the

Hadley circulation that penetrates the lower stratosphere as the 'deep ascending branch. Because the latitudinal location of extreme deep convective zone is higher than the that of oceanic ITCZ, enhancement of convective activity of this continental sector appears as a poleward shift in convective activity in the zonal mean field (Fig. 1b): whereas the climatological OLR peaks around 10°N, the anomalous OLR of the recent period has a maximum around 15°N.

There is a close relationship between the location of the seasonally varying tropical convective active zone and cold tongues in the oceans. Convective activity shifts northward during boreal summer. Accordingly, cross-equatorial winds west of the American and African continents increase, which leads to a decrease in SSTs along coastal regions during boreal summer as a part of a seasonal cycle. The primary cause of cold tongues in tropical SSTs is the shape of the continents, the air–sea interaction, and the location of the rising branch of the Hadley circulation, as described by Xie and Philander (1994) and Xie (2004). We suggest in this paper that changes in the meridional circulation can similarly affect equatorial eastern Pacific SSTs by modulating the cross-equatorial winds, as depicted in Figure 2.

In order to investigate whether the northward shift in the convective zone is driven by the PDO, anomalous OLR during the two periods of neutral and negative phases of the PDO is shown in Fig. 1c and d with anomalous SSTs during those periods (Fig. 1e and f). A characteristic horseshoe pattern in northern Pacific SST is evident during the negative phase of the PDO. Anomalous OLR indicates that convective activity is enhanced along 15° N–20° N irrespective of the phase of the PDO, except for the sector under the direct influence of the PDO in the eastern Pacific, where cooling is greater during the negative phase. However, even during the neutral phase of the PDO, negative anomalies in SST exist in the tropics west of South America. This suggests that SST cooling west of South America is not driven solely by the PDO, but is related to a stronger cross-equatorial winds that we hypothesize is connected to an enhanced convective activity over African-Asian sector.

The atmospheric circulation and SST changes associated with the convective activity are depicted in Fig. 2. The spatial structure of the recent decadal trend varies with the season. The top panels show the 1999–2016 mean anomalous OLR during (a) JAS and (b) OND. Because the response of SST follows the atmospheric circulation, anomalous SSTs during the following month (i.e., August, September and October (ASO) and November, December and January (NDJ)) are displayed in Fig. 2 c and d, respectively. During JAS, the anomalous cross-equatorial flow west of South America intensifies following a poleward shift in convectively active regions. The cross-equatorial flow changes from westward to eastward when it crosses the equator, following the change in sign of the Coriolis force. This results in a strengthening of the climatological easterlies in the SH and enhances anomalous convergence near New Guinea. In contrast, easterlies are weakened in the NH, which explains the warming (cooling) north (south) of the equator. Such a meridional seesaw of anomalous SSTs and cross-equatorial flow suggests an important role for wind−evaporation−SST (WES) feedback (Xie and Philander, 1994) in recent trends. The centre of anomalous negative OLR moves to the equatorial eastern Indian Ocean from boreal summer to autumn,

which results in a strengthening of anomalous easterlies over the equatorial central Pacific and a westward extension of low SSTs over the equator.

3.2 Ascending branch of the Hadley circulation

The Hadley circulation is usually represented by a pair of thermally direct cells, symmetric about the equator, with rising
5 motion over the equatorial belt and sinking motion over the subtropics, with noticeable seasonal variability (e.g., Dima and Wallace, 2003). The mean meridional circulation driven by extreme deep convection further penetrates up to the tropical tropopause (Liu and Zipser, 2005). Here we first investigate the different modes of variability in mean meridional circulation and their relationship with Hadley cells during the boreal summer, focusing on the vertical structure including the lower stratosphere.

Because large detrainment occurs from deep convective clouds near the cloud top, a combination of the vertical velocity and horizontal divergence may indicate large scale circulation related with deep convective activity. Therefore, a singular value decomposition (SVD) analysis (Kuroda, 1998) was conducted using the normalized covariance matrix between zonal-mean pressure vertical velocity (ω) and horizontal air divergence for July-August-September (JAS) 1979-2016. The value at each
15 grid point was weighted by the vertical-layer thickness and the cosine of the latitude in the meridional direction. The SVD calculations were performed from 700 to 30 hPa levels, but to obtain a general view of the entire troposphere the heterogeneous correlation was extended down to 1000 hPa. Results for the 3 SVD leading modes are presented in Fig. 3.

Figure 3a shows that the centers of actions in the divergence field are located in the upper troposphere around 200 hPa for
20 SVD 1 and 3, whereas in the case of SVD 2 it is located around the tropopause at 100 hPa. Accordingly, the vertical velocity fields of SVD 1 and 3 are confined within the troposphere, but that of SVD 2 is extended from the TTL to the lower stratosphere. It is also noticeable that SVD 1 and 3 show similar structure of a meridional seesaw in divergence and vertical velocity fields, except that the horizontal scale of SVD 3 is about a half of the SVD 1.

25 The mass stream function of the climatological residual mean meridional circulation (Kobayashi and Iwasaki, 2016) was examined (Fig. 3a) in order to investigate the correspondence between the climatological Hadley circulation. For convenience, stream lines related to the closed cells in the troposphere, and those extending to the stratosphere (i.e., deep ascending branch) are displayed separately. The results suggest that SVD 1 and 3 represent changes in the strength and meridional shift of the rising branch of Hadley cells. For SVD 2, however, the picture is different: negative values of vertical
30 velocity field in SVD 2 are located along the climatological stream lines connected to the stratosphere, suggesting a strengthening of vertical velocity around the climatological deep ascending branch of the Hadley cell. The different nature of SVD 2 from that of SVD 1 and 3 is also apparent in their time coefficients: an increasing trend is prominent for SVD 2, while for SVD 1 and 3 there is large year-to-year variation. In addition, the amplitude of the interannual variation in the time

series of SVD 1 and 3 show a decadal change. In the case of SVD 1, negative values became smaller from the beginning of the 2000's, whereas in the case of SVD 3 negative values become larger from the end of the 1990's. This almost simultaneous change in the amplitude and a similarity in spatial structure suggest the possibility that a decadal variation of the spatial structure of the same phenomenon is represented by two SVD modes.

Correlation coefficients between the time coefficients of the divergence component of each SVD mode and the OLR, divergence at 925 hPa, and surface (2m) air temperature are shown in Fig. 4. (For easier comparison correlation with SVD 1 time coefficients are displayed above those of SVD 3.) SVD 2 has quite different characteristics compared to SVD 1 and 3: reinforced negative OLR (that is, of convective activity) does not coincide with the region of higher surface temperature as

10 in SVD 1 and 3. Surface temperature does not change, or even decrease in some part over the African-Asian continental sector. It is also noted that enhanced convective zone over the continental sector shows little relationship with the convergence near surface. SVD 1 is easily identified as ENSO related phenomenon with large amplitude in the surface temperature and OLR over the equatorial eastern Pacific. This is in agreement with results from the times series shown in Fig. 3c for SVD 1, which shows that peaks in the time series coincide with the occurrence of the El Niño (dots). Surface

15 temperature and divergence maps of SVD 3 show a meridional seesaw in the tropical northeastern Pacific. Such pattern suggests that SVD 3 is related with the Pacific Meridional mode (PMM) (Chiang and Vimont, 2004) or the Central Pacific ENSO (Stuecker, 2018). The above results support the rationale that the decadal evolution of ENSO-related variation is represented by two SVD modes 1 and 3.

20 The present analysis suggests that the variability of deep ascending zone represented by SVD 2 is a
linearly independent mode from that related to the oceanic ITCZ, represented by SVD 1 and 3. However, the climate system is highly nonlinear. Therefore, changes in the deep ascending branch of the Hadley circulation such as those represented in SVD2, could modulate the ITCZ over the oceanic sector through induced changes in cross-equatorial winds as suggested in Fig. 2.

25 **3.3 Variations over continents and oceans**

In the analysis above, two different features of decadal variability are evident, over oceanic and continental sectors. According to our hypothesis the former corresponds to the variability in oceanic ITCZ constituting the main ascending branch of the Hadley cells, and the latter is related to the deep ascending branches of the Hadley circulation connected to the stratosphere. Here we examine variations over the African continental (10°W–40°E) and Pacific Ocean (170°W–120°W)

30 sectors to reveal the most prominent characteristics in each region. The climatological annual cycle in zonal-mean pressure vertical velocity at 300 hPa for each region are depicted in Figs 5a and 6a. A region of enhanced convective activity migrates north and south over the African continent following the seasonal variation of solar heating (Fig. 5a). It should be noted that the evolution of the convective zone includes a jump during the summer monsoon season (Hagos and Cook, 2007). Over the

Pacific Ocean, the convective zone shows only a small latitudinal displacement and is located in the NH near 5° N–10° N throughout the year (Fig. 6a). Latitude–time cross-sections of the 3-monthly mean anomalous (departures from the 1981-2010 climatology) 300-hPa vertical velocities are shown for February 1979 to November 2016 over the African sector in Fig. 5b. The vertical velocity increases from the mid-1990s in both hemispheres around 10°−20° in latitude, which according to our hypothesis correspond to the location of the deep ascending branch in summertime Hadley circulation. Accordingly, the annual mean precipitation over Africa has increased during the recent period (1999−2016) in both hemispheres over the Sahel and Namibia (Fig. 5c).

Over the Pacific Ocean sector (Fig. 6b), strong upward motion appears over the equator when El Niño events occur. This has been identified as an effect of the ENSO on the ITCZ (Waliser and Gautier,1993). The anomalous region of upward motion, however, tends to remain north of the equator after 1999. Accordingly, the annual mean anomalous precipitation during the recent period shows a large increase near 5° N−10° N, the mean position of the ITCZ over the ocean, but decreases over the equator and the SH (Fig. 6c). This manifests as a narrowing and intensification of the ITCZ in recent decades, with little change in its latitudinal position (Lucas et al., 2013; Wodzicki and Rapp, 2016). The change over the ocean sector is related to the varying strength of the cross-equatorial winds (Fig. 6d). After 1999, although SSTs increased over the equator during El Niño events, anomalous northward winds remained strong and convective activity tended to remain in the NH.

Figure 6e shows the longitude–time section of the anomalous OLR over the equatorial SH (0°–10° S). The effects of cooling of the eastern equatorial Pacific in the SH can also be seen in structural changes in El Niño/Southern Oscillation (ENSO) phenomena after 1999. Convective activity greatly increases over the Pacific during El Niño events before 1999. However, after 1999, Pacific convective activity is suppressed and an increase in convective activity during El Niño is apparent only over the central Pacific. In contrast, convective activity west of 160° E over the Maritime Continent generally increases after 1999. Such changes are likely related to a decadal change in anomalous zonal winds over the tropical SH (10° S−5° N; Fig. 6f), which in turn is connected to increased cross-equatorial southerlies through Coriolis-force effects. Latitude−time sections of 3-monthly anomalous SSTs in the Niño 3.4 sector (Fig. 6g) indicate little change in latitudinal structure, thus changes in spatial structure related to the ENSO around 1999 supports our interpretation of the relationship between SVD 1 and 3 in the above.

We next take a closer look into tropospheric vertical velocity variations. The tropospheric zonal-mean vertical velocity has a relatively weak connection with the horizontal distribution of OLR possibly because regional-scale variations dominate in the lower troposphere due to surface topography. Therefore, meridional sections of standardized mean JAS 1999–2016 anomalous pressure vertical velocity were calculated for several sectors instead of zonal means (Fig. 7). The top panel in Fig. 7a shows the anomalous zonal-mean field (shaded), which is comparable to that extracted by SVD 2 in Fig. 3b, along with contours indicating the 30-yr climatology for reference. The middle panels are the same as the top panel, but divided into

two parts: (b) an African–Asian continental sector (30° W–130° E) and (c) a Pacific–Atlantic oceanic sector (130° E–330° E). A strengthening of upward velocity in the TTL and lower stratosphere occurs in the continental sector, together with a northward shift in the troposphere, whereas in the oceanic sector a strengthening in vertical velocity occurs around 5° N–10° N without a latitudinal shift. If we limit the continental sector to the African continent (20° W–20° E) to exclude the influence of the Indian Ocean, the above-mentioned continental characteristics become even clearer (Fig. 7d). Over the oceanic sector, an increase in vertical velocity occurs around 7.5° N (Fig. 7f), but in the western Pacific sector (130° E–170° E) the upward velocity develops primarily south of the equator (10° S–0°; Fig. 7e). We also note that the climatological vertical velocity in the western Pacific sector is essentially confined to the lower troposphere over the equatorial SH (10° S–0°). This observation can be attributed to the fact that convergence occurs over the warm ocean east of New Guinea (Fig. 2c). This result indicates that despite a variety of profiles among the sectors, the zonal-mean vertical field in the TTL primarily follows variations over the African–Asian continental sector.

3.4 Stratosphere-troposphere coupling

Continuity in a zonally averaged field does not necessarily mean actual continuity at each location, as is evident from the above analysis. To investigate continuity within the deep ascending branch of the Hadley circulation from the upper troposphere to the stratosphere in more detail, longitude−height sections of the normalized anomalous pressure vertical velocities averaged over latitudes of 10°−20° in the summer hemisphere are displayed in the top panels of Fig. 8a and b. The bottom panels show the distributions of climatological (2007−2017) COV occurrence frequency in the same latitudinal zone. If a normal distribution is assumed, absolute values of 17-year mean standardized anomalies that are larger than 0.5 are statistically different from 0 at the 95% confidence level. An increasing trend in upwelling occurs over the continental sector, particularly where COVs are frequent. These characteristics are commonly seen in both summer hemispheres. The contrast between the continental and oceanic sectors is clearer in the SH (Fig. 8b) where the distribution of land is simpler. Because COV occurs in deep convective clouds penetrating into the TTL beyond the level of neutral buoyancy, such increased vertical velocity in the TTL over the region of frequent COV seems reasonable. It should also be noted that a connection between COV and vertical velocity in the tropical lower stratosphere on a daily scale has been identified in a previous study by Kodera et al. (2015).

To investigate stratosphere-related variations in the troposphere, the JAS mean pressure vertical velocity (ω) at 30 hPa averaged over the tropical SH (0°–25° S) is chosen as the index of stratospheric mean meridional circulation (I_ω; Fig. 9a). The correlation coefficient between I_ω and zonal-mean ω at each grid point (Fig. 9b) shows a correlation pattern similar to the SVD 2 in Fig. 1. To highlight the relationship between the interannual variation and climatology, the stream function from Fig. 3 is displayed as contours in Fig. 9b and c. It is clearly seen that the variation in stratospheric upwelling (Brewer–Dobson circulation) is connected to the upwelling of the deep ascending branch of the Hadley circulation, similar to that in climatology.

The correlation between I_ω and zonal-mean temperature at each grid point from 90° S to 90° N is shown in Fig. 9c. Tropical upwelling is not only related to cooling in the tropics and the summer hemisphere, but to warming in the downwelling region around the winter polar stratosphere. This suggests the dynamic nature of recent tropical stratospheric cooling. Stratospheric upwelling is also connected with convective activity along 15° N−20° N (Fig. 9d), as discussed above. Correlation coefficients between I_ω and 925-hPa zonal and meridional winds at each grid point are shown as arrows in Fig. 9e. An increase in cross-equatorial winds in the eastern Pacific and Atlantic is observed. The impact of near-surface wind variations on SST can be seen in the lagged correlation with SST in Fig. 9e. Cooling in the equatorial eastern Pacific is largest with a time lag of 5 months (i.e., during December, January, and February, DJF), consistent with the development of La Niña-like SSTs during boreal autumn (Fig. 2).

On the basis of the results presented in the previous sections we suggest the mechanism depicted in Fig 10. (a) Cooling in the lower stratosphere adds to the global warming in the troposphere. (b) Decrease of the lower stratospheric temperature produced favourable conditions for the development of extreme deep convection. Stratospheric cooling effect is felt by convections reaching the TTL, primarily over the continental sector. (c) Enhancement of extreme deep convection off-equatorial region produces stronger cross-equatorial flow near the surface. (d) Strengthening of surface winds cools the ocean by increased evaporation.

Accordingly, we selected four variables that can be considered fundamental to the recent tropical trends: (a) tropical lower-stratospheric temperatures in early summer (temperature at 70 hPa averaged over 20°S–20°N from 16 July to 16 August); (b) pressure vertical velocity at the bottom of the TTL (150 hPa) in August; (c) August–October mean southward winds south of the equator (10° S–0°) in the western hemisphere (180° W–0°); and (d) time tendency of SST from early summer (May–July) to late autumn (October–December) in the tropical Pacific west of the South American continent (15° S–5° S, 100° W–80° W). Time series of these four variables (a–d) are displayed in Fig 10 (right). When all four variables are negative (red dots), we define this as a negative event. Similarly, when all variables are positive (black dots), it is defined as a positive event. All six positive events occurred within the first 14 years, whereas all seven negative events occurred during the last 13 years. A chi-squared test was conducted to examine whether such distributions of events can occur by chance, by dividing the whole 39 years into three equal 13-year periods. The result ($\chi^2 = 23$) indicates that the probability of such distributions occurring by chance is less than 0.1%. Therefore, there is a statistically significant trend towards negative events in recent decades.

However, the key question here is whether there is a causal relationship among the variables. We introduced a seasonal variation in the selection of the variable from the period of stratospheric cooling at the end of July and to the cooling of the ocean from summer to autumn: That is, change in Pacific SST occurred following a change in cross-equatorial winds,

increased upwelling in the TTL, and stratospheric cooling in early summer. This time evolution tentatively suggests a causality among the variables.

4. Summary and discussion

Convective activity around the deep ascending branch of the boreal summer Hadley circulation (Fig. 3, SVD 2) shows an
5   increasing trend over the continental sector (Fig. 4). In contrast, over the oceanic sector the decadal change manifested as changes in the spatial structure of the ENSO related phenomenon (Fig. 4, SVD 1). It is suggested that the observed 1999-2016 decadal SST cooling in the eastern Pacific is related to an increase in cross-equatorial winds, and easterlies in the tropical SH, which are themselves related to a strengthening of convective activity around the climatological deep ascending branch of the Hadley circulation during boreal summer over the African–Asian sector (Fig. 2). In addition, a correlation
10   analysis (Fig. 9) indicates that these variations in convective activity and SST are related to vertical velocity near the tropopause. The relationship between convective activity and cooling of the tropical eastern Pacific can be explained through changes in cross-equatorial winds involved in a wind−evaporation−SST (WES) feedback (Xie, 2004). Accordingly, a combination of these two processes can be used as a working hypothesis for the recent tropical changes, as shown in Fig. 10.

15   It is difficult to demonstrate statistically a causal relationship among variables having large trends, such as (a) lower stratospheric temperature, (b) upwelling in the TTL, (c) cross-equatorial near-surface winds, and (d) time tendency of SST from boreal summer to autumn. Nevertheless, time lags introduced in selected variables from summer to autumn suggest that the above processes are related, as shown schematically in the left panel of Fig 10.

20   Although their period of observation may be too short (10 years of Atmospheric Infrared Sounder data), Aumann and Ruzmaikin (2013) reported that tropical deep convection over land shows an increasing trend, whereas that over oceans shows a decreasing trend. Furthermore, Taylor et al. (2017) showed that intense mesoscale convective systems in which cloud-top temperatures were lower than −70°C largely increased over the Sahel since 1982. A temperature of −70°C corresponds to the air temperature at ~150 hPa. This means that extreme deep convection penetrating into the TTL largely
25   increased over the African continent, consistent with the analysis presented here.

In the present study, a poleward shift in the convective zone corresponds to enhanced convective activity in the deep ascending branch in the summertime Hadley circulation, located at a higher latitude (around 15° N) than the main ascending branch over the ocean (around 7.5° N). For the purposes of this paper we assume that the changes that we discuss are
30   independent from those associated with tropical expansion. This paper is based on the hypothesis that recent increase in the convective activity in deep branch of the Hadley circulation over the continental sector can be considered as independent of the shift in the ITCZ studied by many other authors such as Schneider (2017) and Byrne et al. (2018) which are primarily

relevant to the oceanic sector. It should also be noted that the expansion rates of the tropics should be much smaller than those reported in past studies (Staten et al., 2018).

The increasing trend in Earth's surface temperature is generally attributed to an increase in greenhouse gases, such as CO_2
5 (IPCC, 2013). Such a change in radiative forcing may explain the global characteristics of recent changes. The effect of increased CO_2 can be divided into a direct radiative effect and an indirect effect through changes in SST. Model experiments have shown that the direct radiative effect of CO_2 increases tropical upward motion, particularly over the Sahelian sector, whereas it suppresses upwelling over the oceanic sector in the Pacific (see fig. 8 of Gaetani et al., 2016). An increase in CO_2 raises the Earth's surface temperature, but decreases stratospheric temperatures. Note, however, that recent cooling in the
10 lower stratosphere–tropopause region is also due to a dynamic effect (Abalos et al., 2015). Further investigation is needed to determine whether the stratosphere is merely passively responding or playing an active role in tropospheric circulation change. Here we emphasized that stratospheric change should be considered together with tropospheric change.

5 Data availability

Datasets used in this paper are all publicly available. Meteorological reanalysis datasets created by JMA (JRA55) are
15 available from http://search.diasjp.net/en/dataset/JRA55. The COBE monthly mean SST dataset can be obtained from the JMA website (http://ds.data.jma.go.jp/tcc/tcc/products/elnino/cobesst/cobe-sst.html). Monthly mean HIRS OLR data can be obtained from NOAA by FTP (ftp://eclipse.ncdc.noaa.gov/cdr/hirs-olr/monthly/). The GPCP monthly mean precipitation dataset can be obtained from the NOAA website (https://www.esrl.noaa.gov/psd/data/gridded/data.gpcp). The AMSU/MHS data are available at NOAA's Comprehensive Large Array Data Stewardship System. In this work, AMSU/MHS raw data
20 were obtained with support from the INSU-CNES French Mixed Service Unit ICARE/climserv/AERIS and accessed with the help of ESPRI/IPSL.

Acknowledgements

The authors wish to express their thanks to Leonhard Pfister for valuable discussions and comments. This work was supported in part by Grants-in-Aid for Scientific Research (25340010, 26281016, and 16H01184) from the Japan Society for
25 the Promotion of Science. Preliminary analysis of this study were made using Interactive Tool for Analysis of Climate System, ITACS, provided by the Japan Meteorological Agency.

References

Abalos, M., Legras, B., Ploeger, F., and Randel, W.J.: Evaluating the advective Brewer-Dobson circulation in three reanalyses for the period 1979–2012, J. Geophys. Res. Atmos.,120, doi:10.1002/2015JD02, 2015.

Adler, R.F., Huffman, G.J., Chang, A., Ferraro, R., Xie, P., Janowiak, J.E., Rudolf, B., Schneider U., Curtis, S., Bolvin. D.T., Gruber, A., Susskind, J., Arkin, P.A., and Nelkin, E.J.: The Version 2 Global Precipitation Climatology Project (GPCP) monthly precipitation analysis (1979-present), J. Hydrometeor, 4, 1147-1167, 2003.

Allen, R.J., Norris, J.R. and Kovilakam, M.: Influence of anthropogenic aerosols and the Pacific Decadal Oscillation on tropical belt width, Nat. Geosci., 7, 270–274, doi:10.1038/NGEO2091, 2014.

Aumann, H.H. and Ruzmaikin, A.: Frequency of deep convective clouds in the tropical zone from 10 years of AIRS data, Atmos. Chem. Phys., 13, 10795–10806, doi:10.5194/acp-13-10795-2013, 2013.

Amaya, D. J., N. Siler, S.-P. Xie, and A. J. Miller, 2018: The interplay of internal and forced modes of Hadley Cell expansion: Lessons from the global warming hiatus. Climate Dyn., 51, 305–319, https://doi.org/10.1007/s00382-017-3921-5, 2018.

Brandt, M., Mbow, C., Diouf, A.A., Verger, A., Samimi, C., and Fensholt, R.: Ground and satellite based evidence of the biophysical mechanisms behind the greening Sahel, Global Change Biol., 21, 1–11, doi:10.1111/gcb.12807, 2014.

Byrne, M.P., Pendergrass, A.G., Rapp, A.D., Wodzicki, K.R.: Response of the intertropical convergence zone to climate change: Location, width, and strength, Curr. Clim. Change Rep., doi.org/10.1007/s40641-018-0110-5, 2018.

Chiang, J., and Vimont, D.: Analogous Pacific and Atlantic meridional modes of tropical atmosphere‐ocean variability, J. Clim., 17, 4143–4158, 2004.

Davis, S.M. and Rosenlof, K.H.: A multidiagnostic intercomparison of tropical-width time series using reanalyses and satellite observations, J. Clim., 25, 1061-1078, 2012.

Diawara, A., Tachibana, Y., Oshima, K., Nishikawa, H., and Ando, Y.: Synchrony of trend shifts in Sahel boreal summer rainfall and global oceanic evaporation 1950–2012, Hydrol. Earth Syst. Sci., 20, 3789–3798, doi:10.5194/hess-20-3789-2016, 2016.

Dima, I., and Wallace, J. M.: On the seasonality of the Hadley Cell, J. Atmos. Sci., 60, 1522-1527, 2003.

Dong, B. and Dai, A.: The influence of the interdecadal Pacific oscillation on temperature and precipitation over the globe, Climate Dyn, 45(9-10):2667–2681, 2015.

Eguchi, N., Kodera, K., and Nasuno, T.: A global non-hydrostatic model study of a downward coupling through the tropical tropopause layer during a stratospheric sudden warming, Atmos. Chem. Phys., 15, 297–304, 2015.

Emanuel, K., Solomon, S., Folini, D., Davis, S., and Cagnazzo, C.: Influence of tropical tropopause layer cooling on Atlantic hurricane activity, J. Clim., 26, 2288–2301, https://doi.org/10.1175/JCLI-D-12-00242.1, 2013.

England, M.H., McGregor, S., Spence, P., Meehl, G.A., Timmermann, A., Cai, W., Gupta, A.S., McPhaden, M.J., Purich, A., and Santoso, A.: Recent intensification of wind-driven circulation in the Pacific and the ongoing warming hiatus, Nat. Clim.Change, 4, 222–227, doi:10.1038/nclimate2106, 2014.

Evan, A.T. and Camargo, S. J. A: climatology of Arabian Sea cyclonic storms, J. Clim.24, 140–158, 2011.

5 Fontaine, B., Roucou, P., Gaetani, M., and Marteau, R.: Recent changes in precipitation, ITCZ convection and northern tropical circulation over North Africa (1979–2007), Int. J. Climatol., 31, 633–648, doi:10.1002/joc.2108, 2011.

Gaetani, M., Flamant, C., Bastin, S., Janicot, S., Lavaysse, C., Hourdin, F., Braconnot, P., and Bony, S.: West African monsoon dynamics and precipitation: the competition between global SST warming and CO_2 increase in CMIP5 idealized simulations, Clim Dyn., doi:10.1007/s00382-016-3146-z, 2016.

10 Gautam, D.K. and Regmi, S.K.: Recent trends in the onset and withdrawal of summer monsoon over Nepal, ECOPERSIA, 1(4): 353-367, 2013.

Hagos, S.M. and Cook, K.H.: Dynamics of the West African monsoon jump, J Clim., 20, 5264–5284. doi:10.1175/2007JCLI1533.1, 2007.

Hong, G., Heygster, G., Miao, J., and Kunzi, K.: Detection of tropical deep convective clouds from AMSU-B water vapor
15 channels measurements, J. Geophys. Res., 110, D05205, doi:10.1029/2004JD004949, 2005.

Hu, S. and Fedorov, A.V.: The extreme El Niño of 2015–2016 and the end of global warming hiatus, Geophys. Res. Lett., 44, doi:10.1002/2017GL072908, 2017.

Hu, Y., Huang, H., and Zhou, C.: Widening and weakening of the Hadley circulation under global warming, Science Bulletin, 63, 640-644, doi:10.1016/j.scib.2018.04.020, 2018.

20 IPCC: Summary for Policymakers. In: Climate Change 2013: The Physical Science Basis. Contribution of Working Group I to the Fifth Assessment Report of the Intergovernmental Panel on Climate Change, Stocker, T.F., Qin, D., Plattner, G.-K., Tignor, M., Allen, S.K., Boschung, J., Nauels, A., Xia, Y., Bex, V., Midgley, P.M. (eds.), Cambridge University Press, Cambridge, United Kingdom and New York, NY, USA, 2013.

Ishii, M., Shouji, A., Sugimoto, S., and Matsumoto, T.: Objective analyses of sea-surface temperature and marine
25 meteorological variables for the 20th century using ICOADS and the KOBE collection, Int. J. Climatol., 25, 865-879, 2005.

Johnson, N.C.: How many ENSO flavors can we distinguish? J. Clim. ,26, 4816–4827, doi:10.1175/JCLI-D-12-00649.1., 2013.

Kajikawa, Y., Yasunari, T., Yoshida, S., and Fujinami, H.: Advanced Asian summer monsoon onset in recent decades, Geophys. Res. Lett., 39, L03803, doi:10.1029/2011GL050540, 2012.

30 Kamae, Y., X. Li, S.-P. Xie, and Ueda, H.: Atlantic effects on recent decadal trends in global monsoon, Clim. Dyn.., doi:10.1007/s00382-017-3522-3, 2017.

Kang, S. M., and Polvani, L.M.: The interannual relationship between the latitude of the eddy-driven jet and the edge of the Hadley cell, J. Clim., 24, 564–568, 2011.

Kao, H-Y., and Yu, J-Y.: Contrasting eastern-Pacific and central-Pacific types of ENSO, J. Clim., 22, 615– 632, doi:10.1175/2008JCLI2309.1., 2009.

Kobayashi, C., and T. Iwasaki: Brewer-Dobson circulation diagnosed from JRA-55, J. Geophys. Res. Atmos., 121, doi:10.1002/2015JD023476, 2016.

5 Kobayashi, S., Ota, Y., Harada, Y., Ebita, A., Moriya, M., Onoda, H., Onogi, K., Kamahori, H., Kobayashi, C., Endo, H., Miyaoka, K., and Takahashi, K.: The JRA-55 Reanalysis: general specifications and basic characteristics, J. Meteorol. Soc. Japan, 93, 5−48, doi:10.2151/jmsj.2015-001, 2015.

Kodera, K., Funatsu, B.M., Claud, C., and Eguchi, N.: The role of convective overshooting clouds in tropical stratosphere–troposphere dynamical coupling, Atmos. Chem. Phys., 15, 6767-6774, doi:10.5194/acp-15-6767-2015, 2015.

10 Kosaka, Y. and Xie, S.-P.: Recent global-warming hiatus tied to equatorial Pacific surface cooling, Nature, 501, 403–407, doi:https://doi.org/10.1038/nature12534, 2013.

Kuroda, Y., An effective SVD calculation method for climate analysis, J. Meteorol. Soc. Jpn., 76, 647-655, 1998.

Lee, H., Gruber, A., Ellingson, R.G., and Laszlo, I.: Development of the HIRS outgoing longwave radiation climate dataset. J. Atmos. Oceanic Technol., 24, 2029–2047, doi: 10.1175/2007JTECHA989.1, 2007.

15 Li, J., Wolf, W.W., Menzel, W.P., Zhang, W., Huang, H., and Achtor, T.H.: Global soundings of the atmosphere from ATOVS measurements: The algorithm and validation, J. Appl. Meteor., 39, 1248–1268, doi.org/10.1175/1520-0450(2000)039<1248:GSOTAF>2.0.CO;2, 2000.

Liu, B. and Zhou, T., Atmospheric footprint of the recent warming slowdown, Scientific Reports, 7, 40947, doi:10.1038/srep40947, 2017.

20 Liu, C. and Zipser, E.J.: Global distribution of convection penetrating the tropical tropopause, J. Geophys. Res.,110, D23104, doi:10.1029/2005JD006063. 2005.

Lucas, C., Timbal, B., and Nguyen, H.: The expanding tropics: A critical assessment of the observational and modeling studies. Wiley Interdiscip. Rev.: Climatic Change, 5, 89–112, doi:10.1002/wcc.251, 2013.

Maidment, R.I., Allan, R.P., and Black, E.: Recent observed and simulated changes in precipitation over Africa, Geophys.
25 Res. Lett., 42, 8155–8164, doi:10.1002/2015GL065765, 2015.

Meehl, G.A., Hu, A., Arblaster, J.M., Fasullo, J., and Trenberth, K.E.: Externally forced and internally generated decadal climate variability associated with the interdecadal Pacific oscillation, J. Clim., 26, 7298–7310, doi:10.1175/JCLI-D-12-00548.1., 2013.

Paek, H., Yu, J.-Y., and Qian, C.: Why were the 2015/2016 and 1997/1998 extreme El Niños different? Geophys. Res. Lett.,
30 44, doi:10.1002/2016GL071515, 2017.

Ramsay, H.: The effects of imposed stratospheric cooling on the maximum intensity of tropical cyclones in axisymmetric radiative–convective equilibrium, J. Clim., 26, 9977–9985, doi: 10.1175/JCLI-D-13-00195.1., 2013.

Randel, W.J. and Jensen, E.J. : Physical processes in the tropical tropopause layer and their roles in a changing climate, Nat. Geosci., 6, 169–176, doi:10.1038/ngeo1733, 2013.

Randel, W.J., Wu, F., Vömel, H., Nedoluha, G.E., and Forster, P.: Decreases in stratospheric water vapor after 2001: links to changes in the tropical tropopause and the Brewer–Dobson circulation, J. Geophys. Res., 111, D12312, doi:10.1029/2005JD006744, 2006.

Seidel, D. J., Q. Fu, W. J. Randel, and T. J. Reichler, 2007: Widening of the tropical belt in a changing climate, Nat. Geosci., 1, 21–24, doi:10.1038/ngeo.2007.38, 2007

Schneider, T.: Feedback of atmosphere-ocean coupling on shifts of the Intertropical Convergence Zone, Geophys. Res. Lett., 44, 11,644–11,653, doi.org/10.1002/2017GL075817, 2017.

Seviour, W.J.M., Butchart, N. and Hardiman, S.C.: The Brewer-Dobson circulation inferred from ERA-Interim, Q. J. R. Meteorol. Soc., 138, 878–888, doi:10.1002/qj.966, 2012.

Staten P.W., Lu J., Grise K.M.,. Davis S.M, and Birner T.: Re-examining tropical expansion, Nature climate change, 8, 768-775, DOI:10.1038/s41558-018-0246-2, 2018.

Stuecker, M. F.: Revisiting the Pacific meridional mode: Sci. Rep., 8, 3216, doi:10.1038/s41598-018-21537-0, 2018.

Taylor, C.M., Belušić, D., Guichard, F., Parker, D.J., Vischel, T., Bock, O., Harris, P.P., Janicot, S., Klein, C., Panthou, G.: Frequency of extreme Sahelian storms tripled since 1982 in satellite observations. Nature, 544, 475–478, doi.org/10.1038/nature22069, 2017.

Trenberth, K. E.: Has there been a hiatus? Science, 349(6249), 691–692, 2015.

Trenberth, K. E., Fasullo, J.T., Branstator, G. and, Phillips, A.: Seasonal aspects of the recent pause in surface warming, Nat. Clim. Change, doi:10.1038/nclimate2341, 2014.

Urabe, Y., Yasuda, T., and Maeda, S.: Rapid warming in global sea surface temperature since around 2013, SOLA, 13, 25−30, doi:10.2151/sola.2017-005, 2017.

Vizy, E.K., and Cook, K.H.: Understanding long‑term (1982–2013) multi‑decadal change in the equatorial and subtropical South Atlantic climate, Clim. Dyn., 46: 2087, doi:10.1007/s00382-015-2691-1, 2016.

Waliser, D.E., and Gautier, C.: A satellite-derived climatology of the ITCZ, J. Clim.,6, 2162–2174, 1993.

Wang, B., Liu, J., Kim, H-J,, Webster, P.J., Yim, S-Y., and Xiang, B.: Northern Hemisphere summer monsoon intensified by mega-El Niño/southern oscillation and Atlantic multidecadal oscillation, Proc Natl Acad Sci U S A, 110, 5347–5352, 2013.

Wang, S., Camargo, S.J., Sobel, A.H., and Polvani, LM.: Impact of the tropopause temperature on the intensity of tropical cyclones—an idealized study using a mesoscale mode, J. Atmos. Sci., 71, 4333–4348, 2014.

Watanabe, M., Shiogama, H., Tabete, H., Hayashi, M., Ishii, M., and Kimoto, M.: Contribution of natural decadal variability to global warming acceleration and hiatus, Nat. Clim. Change, doi:10.1038/nclimate2355, 2014.

Wodzicki, K. R., and A. D. Rapp (2016), Long-term characterization of the Pacific ITCZ using TRMM, GPCP, and ERA-Interim,J. Geophys. Res. Atmos.,121, 3153–3170,doi:10.1002/2015JD024458.

Xiang, B. and Wang, B.: Mechanisms for the advanced Asian summer monsoon onset since the mid-to-late 1990s, J. Clim., 26, 1993–2009, 2013.

Xie, S.-P.: The shape of continents, air-sea interaction, and the rising branch of the Hadley circulation, in The Hadley Circulation, Past, Present and Future, edited by: Diaz, H. F. and Bradley, R. S., Kluwer Academic Publishers, Dordrecht, the Netherlands, 121–152, 2004.

Xie, S.-P. and Kosaka, Y.: What caused the global surface warming hiatus of 1998–2013? Curr. Clim. Change Rep., doi:10.1007/s40641-017-0063-0, 2017.

Xie, S.-P. and Philander, S.G.H.: A coupled ocean-atmosphere model of relevance to the ITCZ in the eastern Pacific, Tellus, 46A, 340−350, 1994.

Yun, K.-S., Lee, J.-Y., and Ha, K.-J.: Recent intensification of the South and East Asian monsoon contrast associated with an increase in the zonal tropical SST gradient, J. Geophys. Res. Atmos., 119, 8104–8116, doi:10.1002/2014JD021692, 2014.

Figures
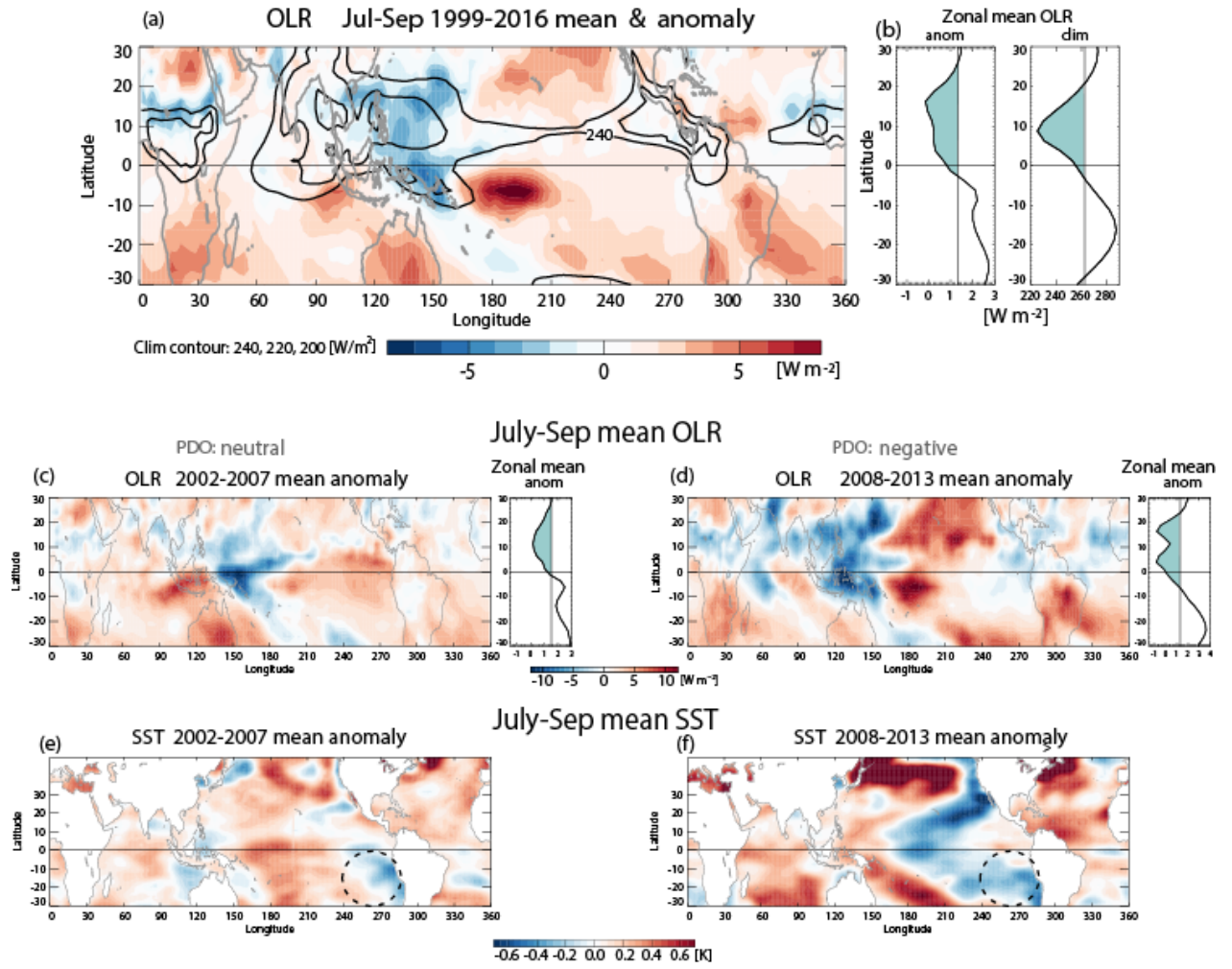
Figure 1: (a) Climatological (1981–2010) July–September mean OLR (contours: 240, 220, and 200 W m⁻²) and anomalous July–September OLR (departures from climatology) during 1999–2016 (colour shading); **(b)** zonal-mean profiles of (a): anomalies from climatology (left) and climatology (right); **(c)** anomalous OLR as in (a) and (b, left) but for 2002–2007; **(d)** anomalous OLR as in (a) and (b, left) but for 2008–2013; and anomalous July–September SST (departures from climatology) for **(e)** 2002–2007 and **(f)** 2008–2013.
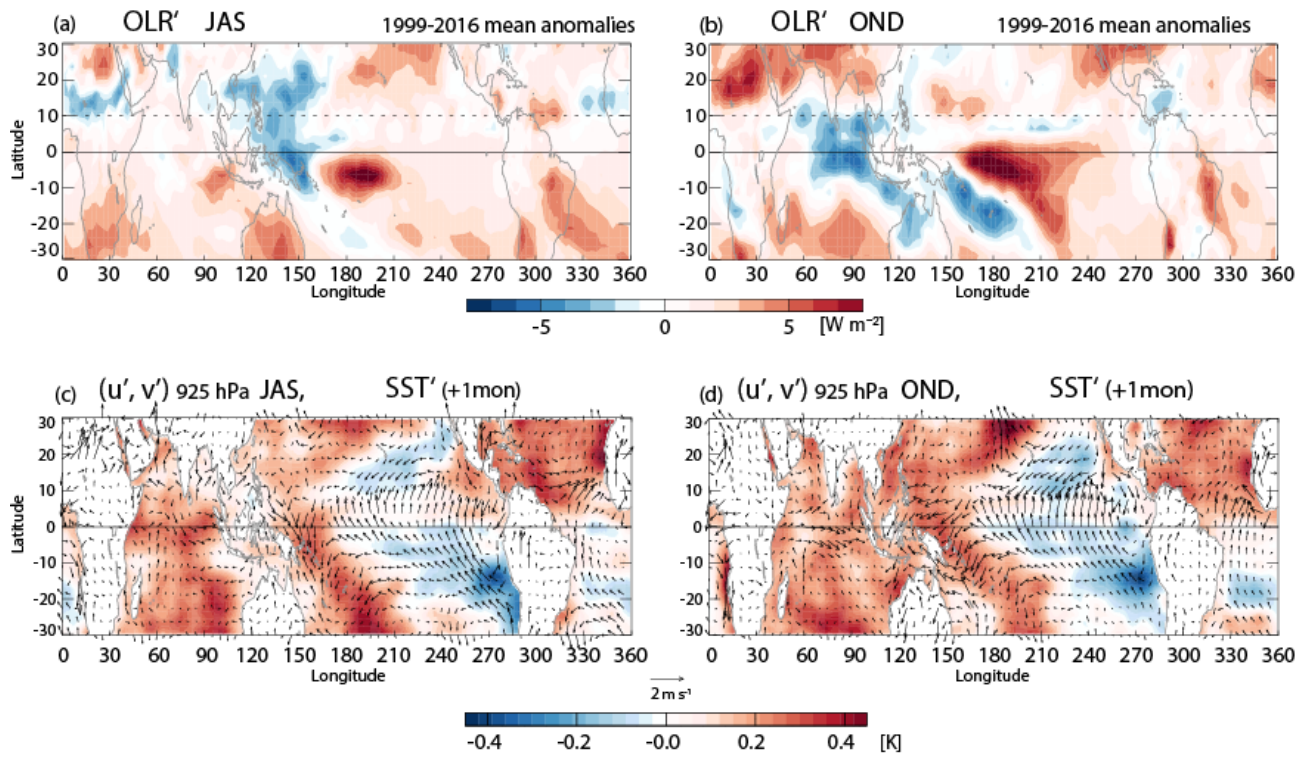
Figure 2: (a) JAS and (b) OND mean anomalous OLR for 1999–2016; (c) JAS and (d) OND mean anomalous horizontal winds at 925 hPa (arrows) for 1999–2016 superimposed on anomalous SSTs (colour shading) with a one-month lag (i.e., ASO and NDJ, respectively).
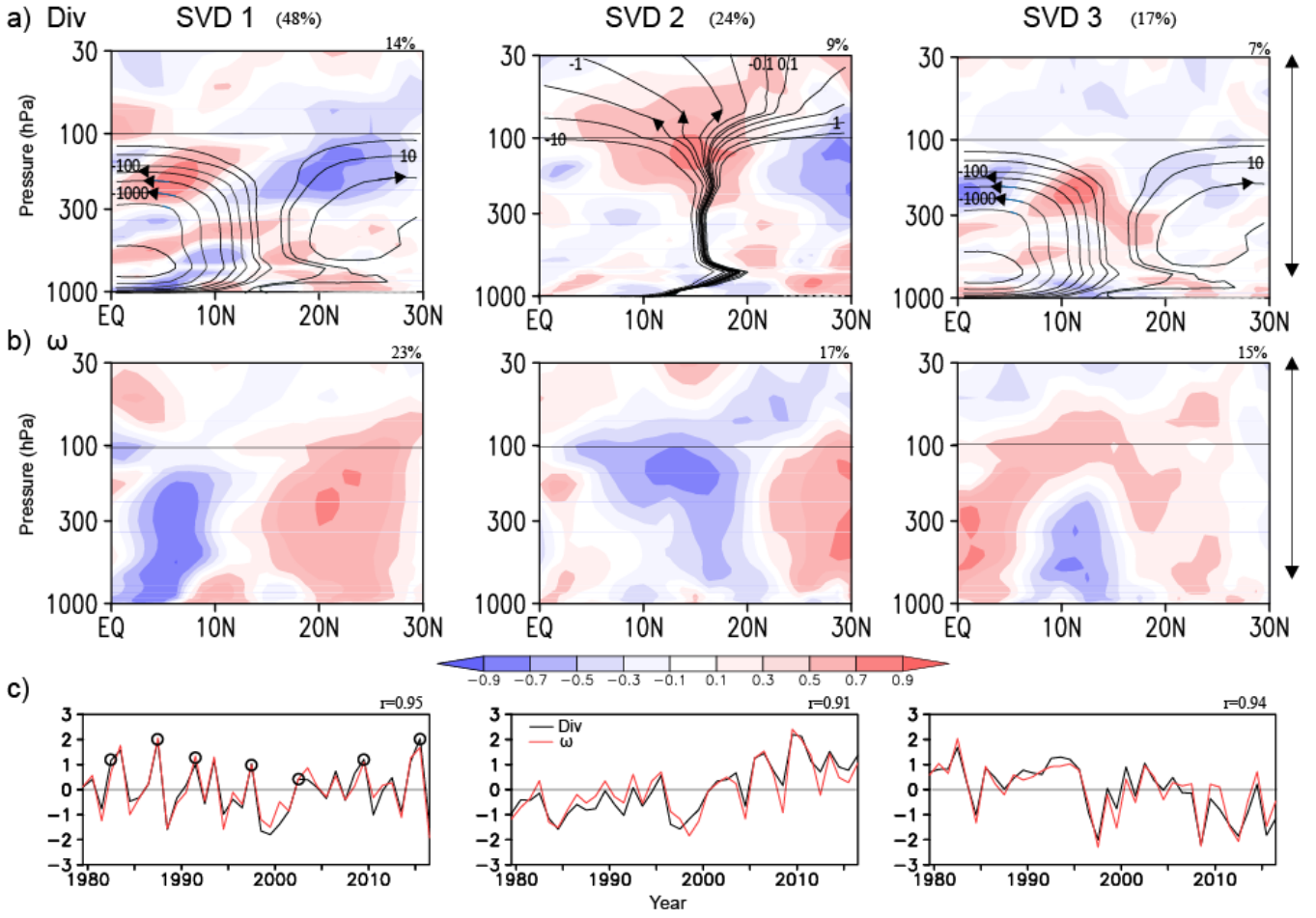
Figure 3: Singular value decomposition analysis of the zonal-mean anomalous horizontal divergence and anomalous pressure vertical velocity in the tropics (30°S–30°N) during JAS from 1979 to 2016: From left to right, SVD 1, SVD 2 and SVD 3. (a) Heterogeneous correlation map of horizontal divergence. (b) same as (a), except for pressure vertical velocity map. (c) Time coefficients (black: divergence, red: vertical velocity). Arrows indicate the levels used in the SVD calculations. Stream lines in (a) indicate mass stream function of the climatological residual mean meridional circulation (Stream lines are plotted with logarithmic scaling: ± 0.1, 0.2, 0.5, 1, 2, 5, 10, 20, 50, 100 ... × 10^{10} kg s^{-1}). Open circles in (c) indicate El Niño event.
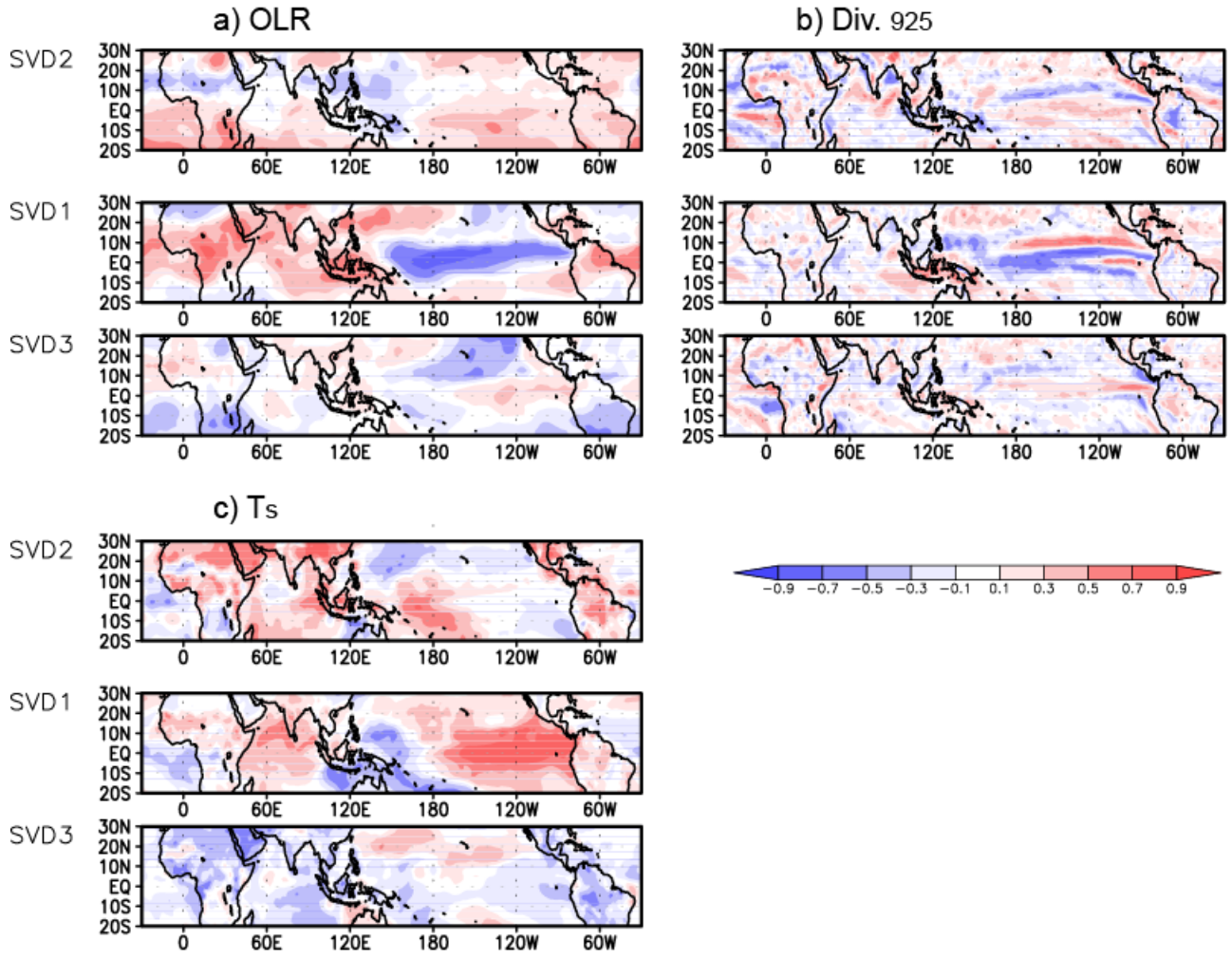
Figure 4: Correlation coefficient between time series of divergence component of each SVD mode and (a) OLR, (b) horizontal divergence at 925 hPa, and (c) surface temperature, at each grid. Each panel in Fig. a, b, and c shows correlation map of SVD 2, SVD 1, and SVD 3, from top to bottom.
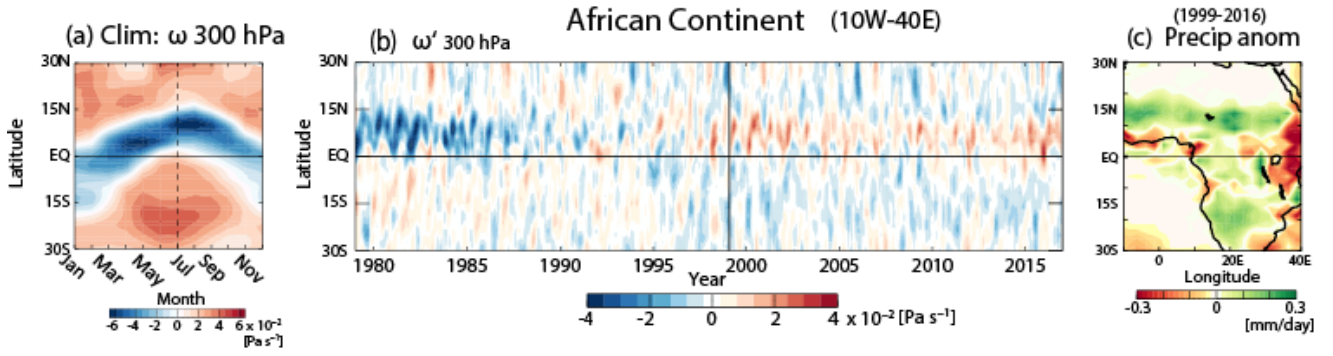
Figure 5: (a) Latitude–time section of the climatological zonal-mean pressure vertical velocity at 300 hPa averaged over the African sector (10°W–40°E); **(b)** latitude–time section of monthly mean anomalous pressure vertical velocity from February 1979 to November 2016; and **(c)** latitude–longitude map of annual mean anomalous precipitation during 1999–2016 over the African sector. A three-month running mean is applied in (b).
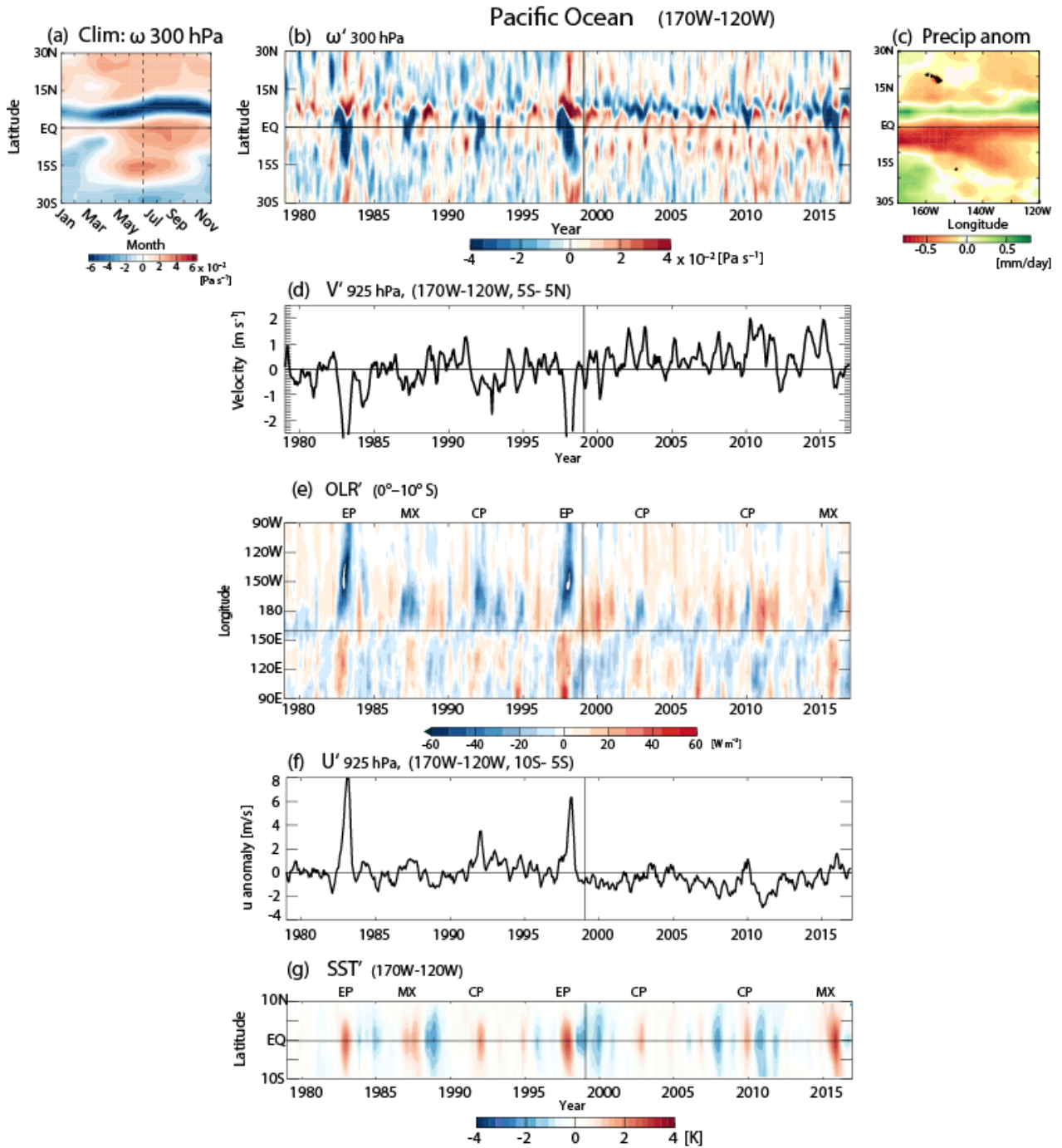
Figure 6: (a–c) Same as Fig. 5 but for the eastern Pacific Niño-3.4 (170°W–120°W) sector; (d) monthly mean anomalous meridional wind component around the Equator (5°S–5°N) over the Niño 3.4 sector; (e) similar to (a), but for the time–longitude section of OLR around the Equator (5°S–5°N) over the Indian Ocean–Pacific sector; (f) same as (d), but for the zonal wind component in the tropical SH (10°S–5°S); and (g) monthly mean anomalous SST over the Nino 3.4 sector. Eastern Pacific (EP), central Pacific (CP), and mixed-type (MX) El Niño events are indicated (Paek et al., 2017).
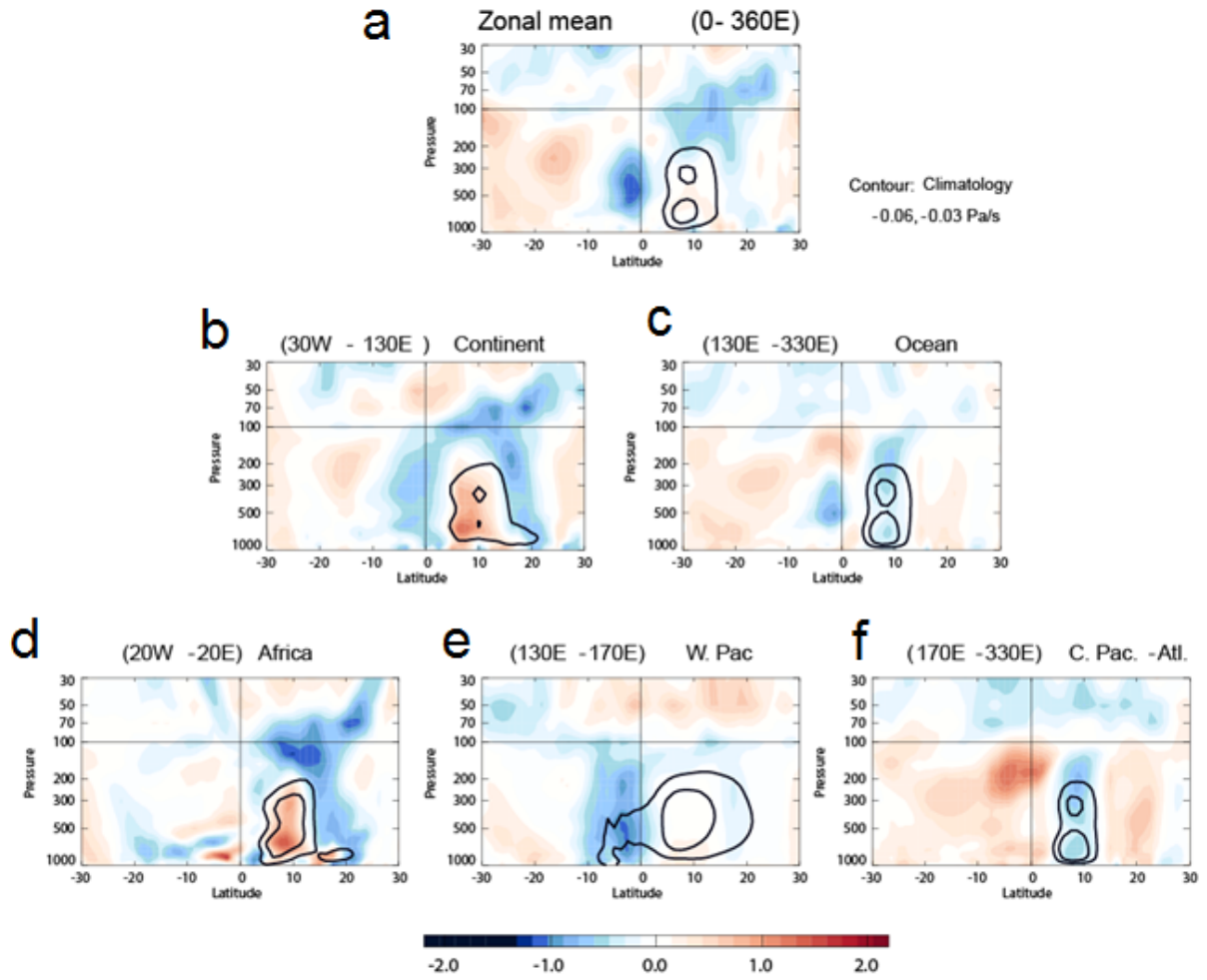
Figure 7: (a) Standardized anomalous pressure vertical velocity (departures from 1981–2010 climatology)—the climatological JAS mean, zonal-mean pressure vertical velocity is indicated by contours (–0.06 and –0.03 Pa s⁻¹). (middle panels) Same as (a), but for **(b)** the African–Asian continental sector (30°W–130°E) and **(c)** the Pacific–Atlantic oceanic sector (130°E–330°E). (bottom panels) same as (a), but for **(d)** the African continental sector (20°W–20°E), **(e)** the Western Pacific sector (130°E–170°E), and **(f)** the Central Pacific–Atlantic sector (170°E–330°E).
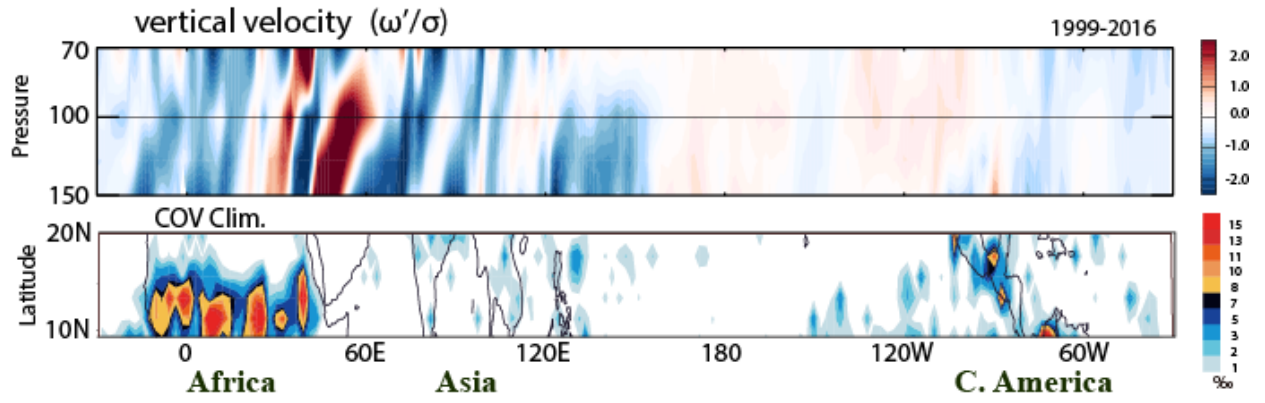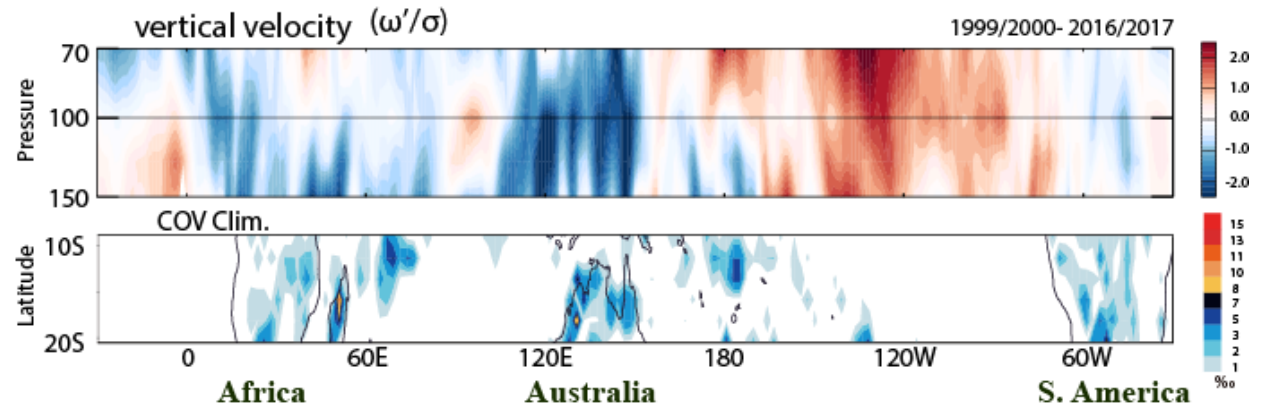
Figure 8: (a) (top) Height–longitude section of the standardized (with respect to the interannual variation) anomalous pressure vertical velocity averaged over 10°N–20°N during boreal summer (JAS) 1999–2016; (bottom) climatological (2007–2017) occurrence frequency of convective overshooting (COV) in the same latitudinal zone (units of parts per thousand); and (b) as in (a) but for 10°S–20°S during austral summer (DJF).
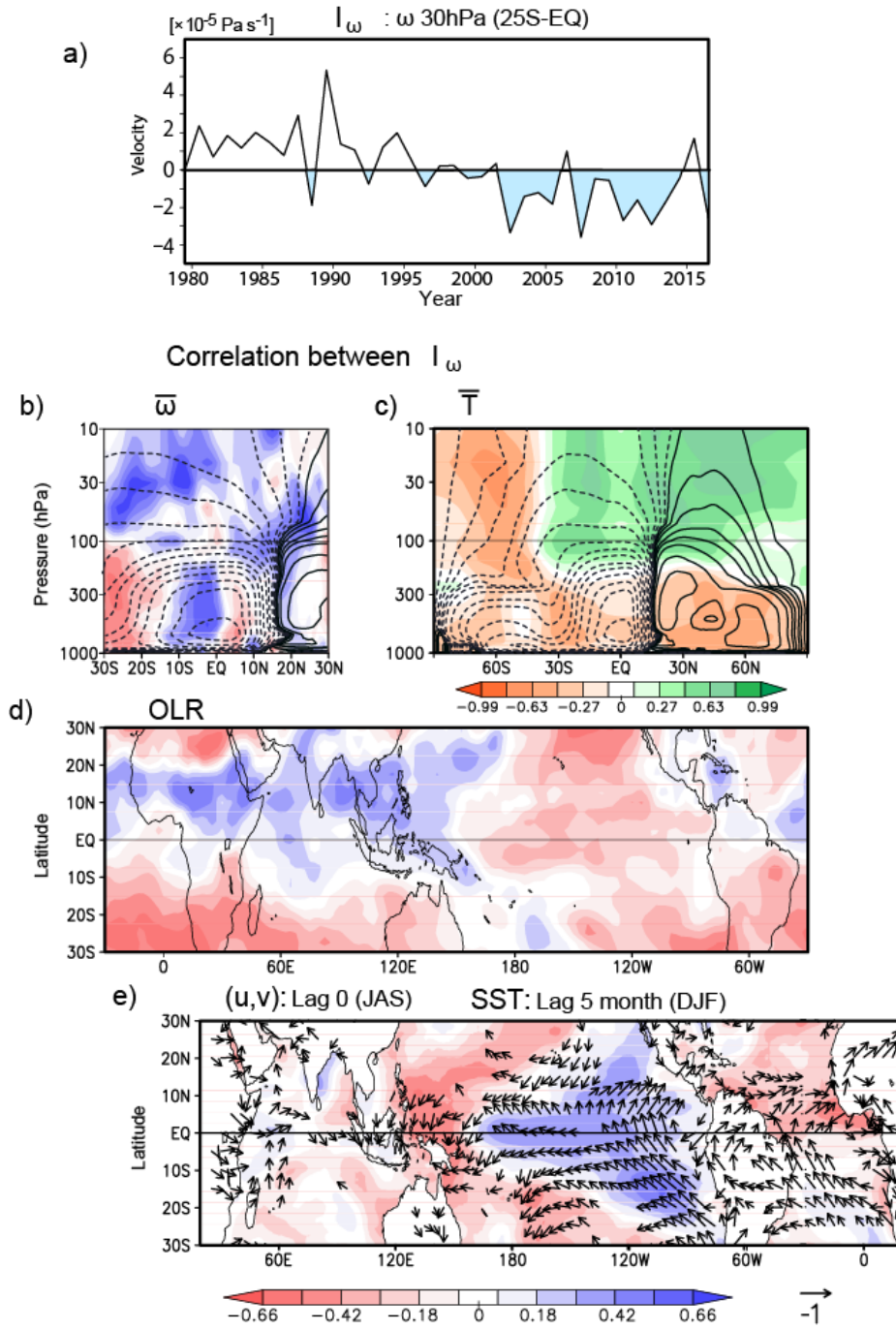
Figure 9: (a) Time series of JAS mean pressure vertical velocity (ω) at 30 hPa averaged over 0°–25°S as an index for tropical stratospheric vertical velocity (I_ω); correlation coefficients between I_ω and **(b)** zonal-mean ω, **(c)** zonal-mean temperature T at each grid, **(d)** OLR, and **(e)** horizontal winds at 925 hPa (arrows). A lagged correlation with DJF mean SST is also presented by colour shading in (e). Contours in (b) and (c) indicate the climatological residual mean meridional circulation in JAS. Solid and dashed lines indicate clockwise and counter clockwise directions, respectively.
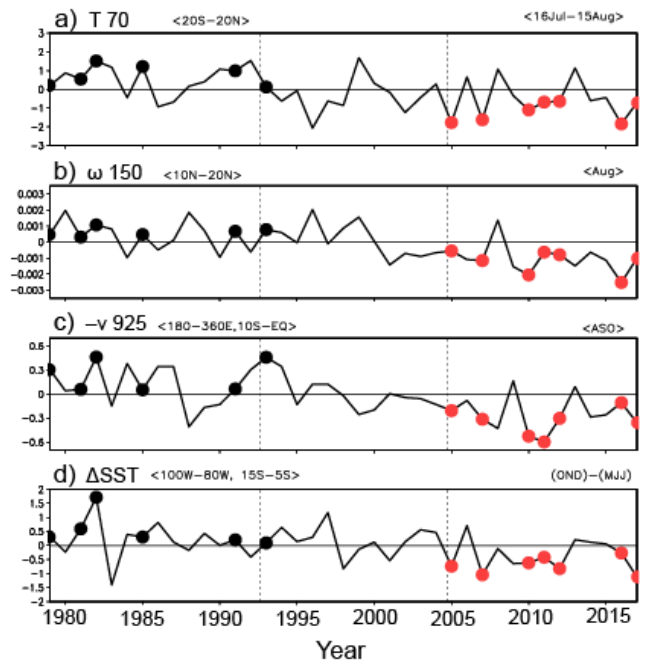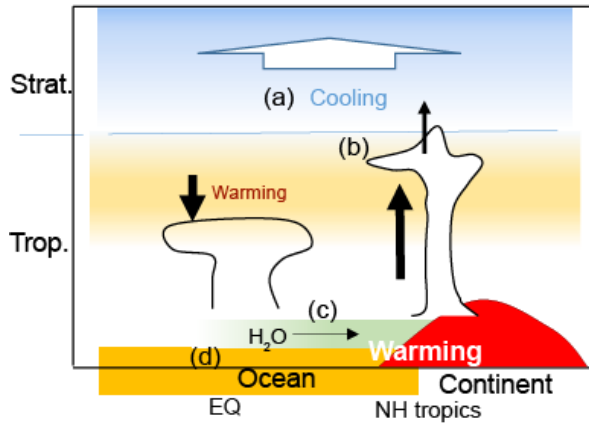
Figure 10: (left) Schematic of recent changes in the tropics (see text), in which the labels (a) to (c) indicate the location of the variable shown in the right panels; (right) time series of four key variables as departures from the climatology: (a) lower stratospheric temperature, (b) upwelling in the TTL, (c) cross-equatorial near-surface winds, and (d) time tendency of SST from summer to autumn. Black and red dots indicate years when the four variables are of the same polarity (positive and negative, respectively).